



## Sustainable Production of ZnO Nanoparticles from *Trianthema Portulacastrum* and Their Efficacy against Pathogenic Microbes

A. KASTHURI<sup>1</sup>, K. K. ILAVENIL<sup>2\*</sup>, P. PANDIAN<sup>3</sup> and R. PUNITHA<sup>4</sup>

<sup>1,4</sup>Department of Chemistry, Nehru Memorial College (Autonomous)/Affiliated to Bharathidasan University, Puthanampatti-621 007, Tiruchirappalli, Tamilnadu, India.

<sup>2\*</sup>Department of Chemistry, School of Engineering and Technology, Dhanalakshmi Srinivasan University, Samayapuram, Tiruchirappalli-621112, Tamilnadu, India.

<sup>3</sup>Department of Chemistry, Thanthai Periyar Government Arts and Science College (Autonomous)/Affiliated to Bharathidasan University, Tiruchirappalli-620023, Tamilnadu, India.

\*Corresponding Author: ilavenilkk.set@dsuniversity.ac.in

<http://dx.doi.org/10.13005/ojc/420111>

(Received: June 06, 2025; Accepted: August 07, 2025)

### ABSTRACT

This research investigates the eco-friendly manufacture of zinc oxide nanoparticles utilising the leaf extract of *Trianthema portulacastrum*, a medicinal plant recognized for its bioactive phytochemicals. The synthesis process avoids harmful ingredients, conforming to sustainable and environmentally responsible procedures. Thorough structural and chemical evaluations utilising FTIR, UV-Vis spectroscopy, SEM, DLS, and XRD confirmed the successful production of stable ZnO nanoparticles, which have a distinct hexagonal wurtzite crystal structure and surfaces functionalized by plant-derived proteins. The UV-Vis spectrum exhibited a red-shifted absorption, signifying distinctive optical characteristics. The DLS data indicated moderate aggregation with a hydrodynamic diameter of approximately 97.8nm. The antibacterial efficiency was assessed against various pathogenic strains, demonstrating substantial inhibitory zones, particularly surpassing traditional medications in effectiveness against *Mycobacterium tuberculosis*.

**Keywords:** Zinc oxide nanoparticles, Green synthesis, *Trianthema portulacastrum*, UV-visible spectroscopy, Antimicrobial activity, Phytochemicals.

### INTRODUCTION

Nanomaterials (NMs) derived from natural sources have emerged as a result of the growing need for environmentally friendly materials. NMs are utilised in a variety of sectors, including medicine, biosensors, and catalysts,

due to their nanoscale size and significantly larger surface area. The conventional methods of synthesis frequently involve the use of hazardous chemicals and a significant amount of energy, which can be hazardous to both the environment and human health. Green synthesis, on the other hand, makes use of natural reagents such as plant



extracts and microorganisms, and thus provides an option that is both friendly to the environment and economical. This method is said to be a promising strategy for the production of non-toxic metal oxide nanoparticles, and it is in accordance with the principles of green chemistry. Because of its one-of-a-kind characteristics and applicability in a wide range of sectors, including biomedicine, electronics, and catalysis, zinc oxide nanoparticles are the subject of much research<sup>1</sup>. Their significant antibacterial and anti-inflammatory activities suggest potential as viable substitutes for traditional antibiotic therapies. Replacing traditional chemical methods with green synthesis approaches for metal oxide nanoparticles promotes sustainability and reduces environmental impact. The conventional method of chemical synthesis frequently includes the use of dangerous chemicals and toxic solvents<sup>2,3</sup>, and it necessitates the application of high temperatures and pressures, which eventually results in environmental contamination and health dangers. Physical and chemical methods can synthesize nanoparticles with precise particle size and shape for specific purposes. Infrared irradiation, pulsed laser deposition, sol-gel processing, thermal evaporation<sup>4</sup>, microwave-assisted synthesis<sup>5</sup>, chemical vapor deposition<sup>6</sup>, electrochemical reactions, and sputtering<sup>7</sup> are some of the techniques that are commonly used. The green synthesis method, on the other hand, makes use of biological resources such plant extracts, bacteria, fungi, and algae, all of which serve as natural reducing and stabilizing agents. This strategy functions in ambient conditions, so reducing the amount of energy that is consumed and doing away with the requirement for potentially hazardous compounds<sup>8</sup>. Therefore, green synthesis results in the production of nanoparticles that are non-toxic and biocompatible. This is in accordance with the principles of green chemistry and promotes safer uses in a variety of disciplines, including medicine and environmental cleanup.

The green synthesis of zinc oxide nanoparticles (ZnO-NPs) has been produced using plant extracts rich in phytochemicals, including flavonoids and phenolics, which serve as natural reducing and stabilising agents<sup>9</sup>. A cost-effective and environmentally responsible alternative to conventional procedures, this eco-friendly approach is in line with the principles of

green chemistry. ZnO-NPs provide antibacterial effects by forming reactive oxygen species (ROS), releasing Zn<sup>2+</sup> ions, and directly contacting microbial cell membranes<sup>10</sup>. Several different pathogens are effectively inhibited as a result of these actions, which affect the structures and functions of the cells. Due to this, green-synthesized ZnO-NPs have the potential to be utilized in a variety of applications, including the treatment of cancer<sup>11-12</sup>, antimicrobial therapy<sup>13</sup>, wound healing<sup>14</sup>, and environmental clean-up. Temperature, pH, and precursor concentration greatly affect zinc oxide (ZnO) nanostructure shape. These conditions can change ZnO's physical and chemical properties. It has a high aspect ratio, big surface area, and considerable optical and electrical properties<sup>15</sup>.

ZnO NPs show significant antibacterial action against several *Gram-positive* and *Gram-negative* microorganisms. *Staphylococcus aureus*, *Escherichia coli*, *Pseudomonas aeruginosa*, *Klebsiella pneumoniae*, and *Bacillus subtilis* are vulnerable to ZnO NPs. The broad-spectrum antibacterial properties of these nanoparticles make them viable bacterial infection treatments<sup>16</sup>. Notably, their efficacy persists even in the absence of light, attributed to mechanisms such as reactive oxygen species generation, membrane disruption, and zinc ion release<sup>17</sup>. ZnO nanoparticles are a promising alternative to conventional antibiotics, particularly when it comes to combating drug-resistant bacteria, due to the qualities that they possess. Their physicochemical properties, on the other hand, might change depending on the conditions of the surrounding environment. Furthermore, in larger concentrations, they may present a hazard to living species and ecosystems. Nanoparticles of zinc oxide (ZnO) have been successfully synthesised using *Trianthemaportulacastrum* leaf extract, which is environmentally friendly. The natural phytochemicals of the plant, such as flavonoids, phenolic compounds, terpenoids, and alkaloids, are utilised in this environmentally friendly approach. These phytochemicals fulfil the roles of reducing and stabilising agents during the synthesis process. In the realms of biological and environmental cleanup, the ZnO nanoparticles that emerge as a result show intriguing uses.

### Sharunai plant

Aizoaceae member *Trianthema portulacastrum* known as huge pigweed, black pigweed, desert horse purslane, or Olowonjeja. Although its origin is unknown, it is found in tropical and subtropical locations including Africa, India, Southeast Asia, West Asia<sup>18</sup>, southern China, and tropical America. Traditional Ayurvedic medicine uses *T. portulacastrum* for treatment. It is used in herbal cough, uteralgia, and inflammatory therapies. It is also valued as a green vegetable in the diets of economically disadvantaged populations in the Indian subcontinent<sup>19</sup>. The plant is known by various vernacular names in India, including Bishkhapraor Safed Bishkhaprain Hindi, Gaddicherakuor Kotthimeeraakuin Telugu, Sarunai Keeraior Thotta Keeraian Tamil, Attum Parippuin Malayalam, Elachikkiraor Garikain Kannada, and Shukhatarain Marathi. Traditionally, the plant has been used for treating edema in the liver and spleen, uteralgia, and cough. It is considered lithotriptic for the kidney and bladder and is widely recognized in Indian traditional medicine as a diuretic. Studies have demonstrated its hepatoprotective activity, particularly against paracetamol and thioacetamide-induced intoxication in rats<sup>20</sup>. Terpenoids, phenolic chemicals, alkaloids, saponins, and flavonoids have been found in *Trianthema portulacastrum* phytochemical studies. Antioxidant, Anti-inflammatory, Analgesic, and Anti-infective properties characterise these components. An increasing number of *in vitro* and *in vivo* research show that the plant can prevent or treat hepatotoxicity, nephrotoxicity, hyperglycemia, hyperlipidaemia, infectious illnesses, and cancer. Notable chemical components of the plant<sup>21</sup> include 15-hydroxymethyl-2,6,10,18,22,26,30-heptamethyl-14-methylene-17-hentriacontene (commonly known as trianthenol), ketoconazole, glibenclamide, 3-methoxy-4-hydroxybenzoic acid, N-nitrosodiethylamine, aflatoxin B1, miconazole, phenobarbital, bilirubin, and 3,7-dihydro-1,3,7-trimethyl-1H-purine-2,6-dione<sup>22</sup>. *Trianthemaportulacastrum* is used to treat eye-related issues<sup>23</sup>.

### Methodology

#### Preparation of *Trianthemaportulacastrum* leaf extract

Fresh leaves of *Trianthema portulacastrum*

were collected and meticulously rinsed with distilled water to eliminate surface contaminants prior to preparing the dry leaf powder for aqueous extraction. The cleansed leaves were subsequently shade-dried in a well-ventilated environment to retain heat-sensitive phytochemicals. After thorough drying, the leaves were pulverised into a fine powder with a mechanical grinder and sifted to achieve consistent particle size. The resultant powder was preserved in sealed containers to avert moisture absorption and deterioration. During the extraction process, 30 g of the produced leaf powder were subjected to boiling in 100 mL of distilled water for 1 h to promote the release of bioactive components. Subsequent to boiling, the mixture was allowed to cool to ambient temperature and then filtered with Whatman No. 44 filter paper to isolate the solid residues from the liquid extract. The filtrate underwent additional purification via centrifugation, and the resultant clear supernatant was meticulously collected and preserved at 4°C for subsequent analysis or experimental applications.

#### Nanoparticle Zinc Oxide Synthesis

The nanoparticles were synthesised using *Trianthemaportulacastrum* leaf powder and 0.03 M zinc sulphate heptahydrate ( $\text{ZnSO}_4 \cdot 7\text{H}_2\text{O}$ ) as the zinc precursor in a green reflux method. The aqueous plant extract was made by boiling 10 g of air-dried leaf powder in 250 mL of distilled water at 80°C for 1 h with steady agitation. Zinc sulphate heptahydrate was dissolved in 100 mL of distilled water with continuous stirring to create a 0.03 M zinc sulphate solution. Subsequently, 25 mL of the produced plant extract was incorporated into the zinc sulphate solution while maintaining continuous agitation. While stirring, 0.1 M sodium hydroxide (NaOH) solution was added dropwise to adjust the liquid's pH to 10. After refluxing at 80-90°C for 3 h, the solution reduced zinc ions and synthesised ZnO nanoparticles, with phytochemicals from the plant extract acting as reducing and stabilising agents. After reflux, the mixture cooled to room temperature and was centrifuged at 10,000 rpm for 15 min to separate nanoparticles. To remove impurities, the pellet was cleaned with distilled water and ethanol, then dried in a 60°C hot air oven for 12 hours.

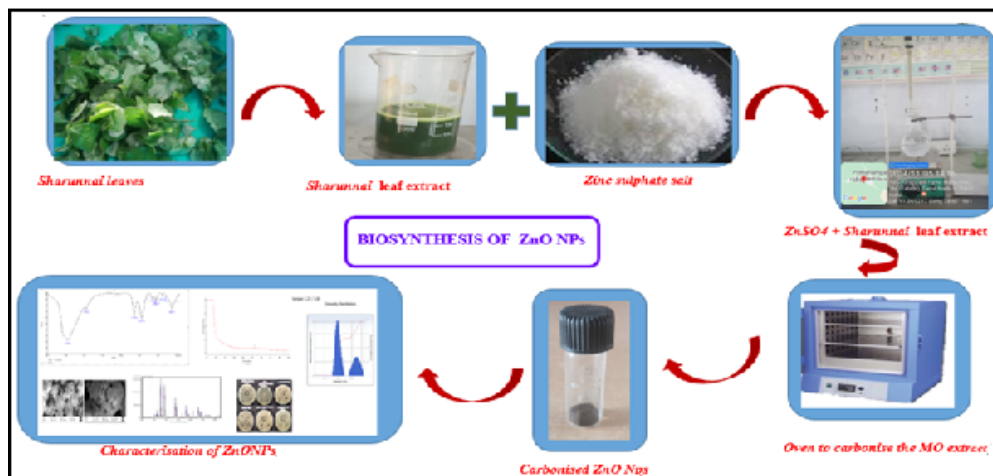


Fig. 1. Biosynthesis of *Trianthema portulacastrum*- ZnONPs

**Chemical Profiling of Medicinal Plant**

The phytochemical analysis of primary and secondary metabolites in medicinal plants utilises various traditional methodologies. The Fehling's carbohydrate test was conducted by combining equal volumes of leaf extract with Fehling's A and B reagents, followed by heating for 3-5 min until a crimson precipitate formed, signifying the presence of reducing sugars<sup>24</sup>. The iodine test for starch involved mixing 2 mL of *Trianthema portulacastrum* leaf extract with iodine and potassium iodide (Lugol's solution), producing a blue hue that signifies the presence of

starch. The Biuret test for proteins was conducted by combining 1 mL of leaf extract with 3% zinc sulphate and 10% sodium hydroxide, yielding a violet or red colouration, indicative of the presence of proteins or peptides. Salkowski's test for steroids was employed to identify secondary metabolites, wherein *Trianthema portulacastrum* leaf extract was mixed with chloroform, followed by the addition of sulphuric acid, yielding a crimson hue indicative of steroids<sup>25</sup>. The alkaloids test by Wagner involved mixing the leaf extract with potassium iodide and iodine solution, resulting in a precipitate that signified the presence of alkaloids.<sup>26</sup>

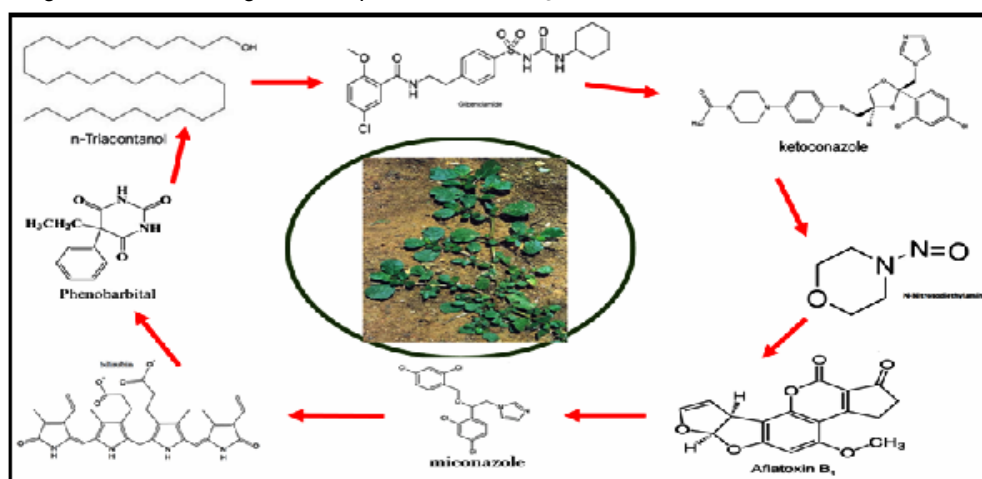


Fig. 2. Phytochemicals in *Trianthema portulacastrum*

**RESULTS AND DISCUSSION**

**Functional group analysis**

The FTIR spectra of the synthesised ZnO nanoparticles exhibits peaks at 3432.53 cm<sup>-1</sup> (O–H

stretching), 3209.64 cm<sup>-1</sup> (N–H stretching), and 2927.26 cm<sup>-1</sup> (C–H stretching), signifying the presence of hydroxyl, amine, and aliphatic groups from plant-derived biomolecules. The signal at 1646.02 cm<sup>-1</sup> indicates C=O stretching, implying the presence of

amide or carboxylic groups. Supplementary peaks at 1484.58 cm<sup>-1</sup> and 1401.77 cm<sup>-1</sup> are ascribed to aromatic C–C stretching and carboxylate groups, respectively. The bands at 1307.07 cm<sup>-1</sup> and 1083.61 cm<sup>-1</sup> signify C–N and C–O stretching vibrations, indicating the presence of amines and alcohols. Peaks at 880.26 cm<sup>-1</sup> and 778.56 cm<sup>-1</sup> correspond to out-of-plane bending of =C–H in alkenes, while peaks at 693.2, 617.95, 511.24, and 464.45 cm<sup>-1</sup> are indicative of Zn–O stretching vibrations, thereby validating the creation of ZnO nanoparticles. The results indicate that phytochemicals from the plant extract function as reducing and capping agents, hence stabilising the ZnO nanoparticles during production.

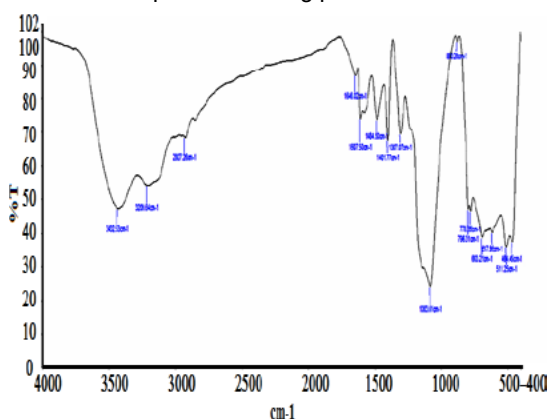


Fig. 3. FTIR spectrum of Tp-ZnO

**UV-Vis absorbance spectrum**

An absorption peak at 613.6nm in the UV-Vis spectra of zinc oxide (ZnO) nanoparticles is unusual, as pure ZnO generally displays a prominent absorption peak about 375nm owing to its large band gap of approximately 3.3 eV. The detected red-shifted absorbance at 613.6nm indicates alterations in the structure or composition of the ZnO nanoparticles.

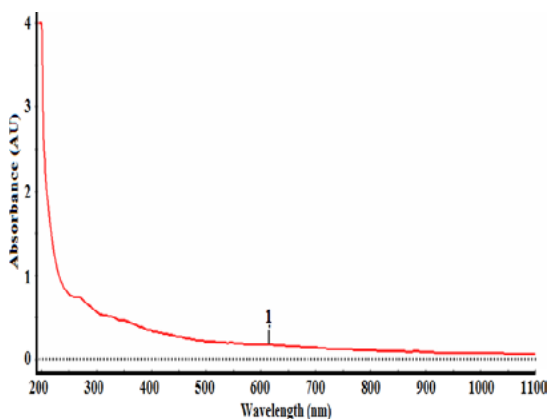


Fig. 4. UV-Visible spectrum of Tp-ZnONPs

**Hydrodynamic Size Determination via DLS**

Dynamic Light Scattering examination of zinc oxide nanoparticles synthesised from *Trianthemaptortulacastrum* leaf extract showed a hydrodynamic diameter of 97.8nm, a PDI of 0.285, and a diffusion constant of 5.029×10cm<sup>2</sup>/s. According to the PDI, the particles are mostly evenly spread out, indicating a fairly monodisperse distribution. It's likely that the stated average size of 134.2nm is an intensity-weighted mean, which means that it can be changed by bigger particles or groups of particles, since DLS measurements are sensitive to these kinds of changes.

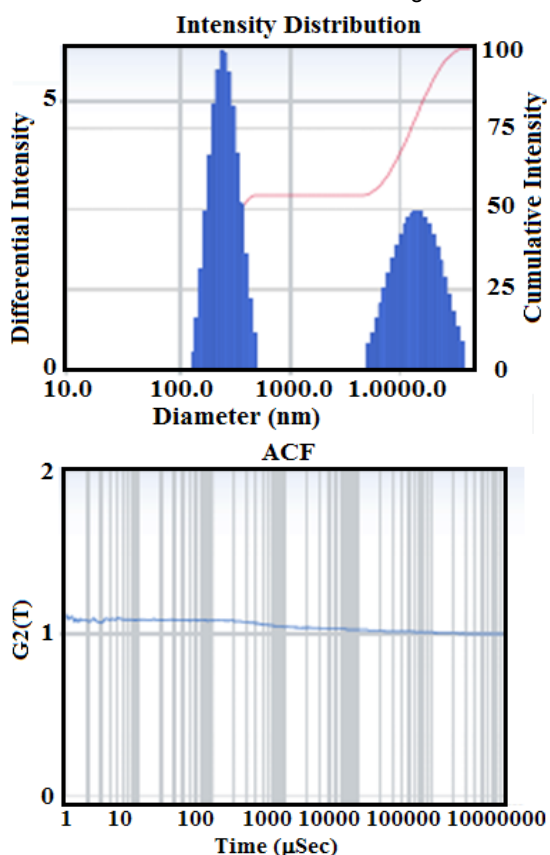
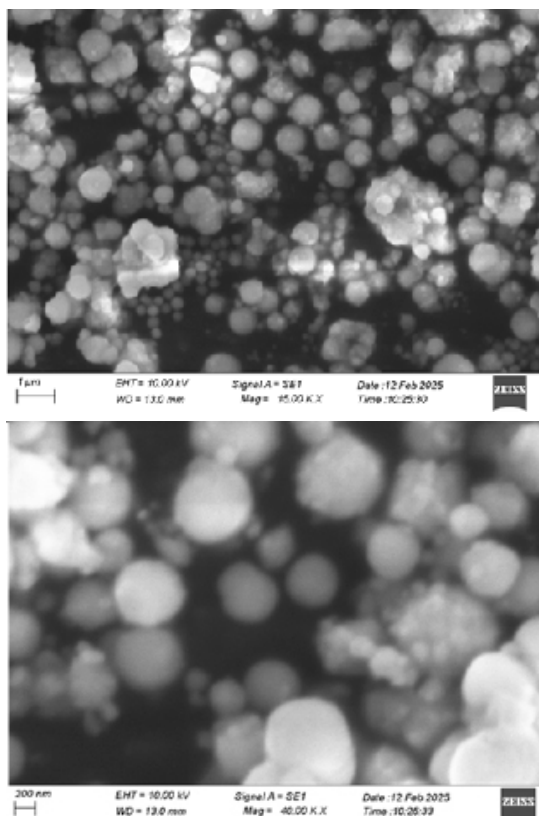


Fig. 5. DLS of Tp-ZnONPs

**Morphological Features of ZnO Nanoparticles**

To further characterise the ZnO NPs, their appearance and structure were examined using SEM. Fig. 6 depicts ZnO nanoparticles with a particle-like morphological appearance and a spherical shape with a uniform size distribution, as described in the literature<sup>27</sup>. Nanoparticles agglomerate and cluster as a direct result of their high surface energy.



**Fig. 6. SEM images of Tp- ZnO NPs at 1 μm and 2 μm Crystallographic Characterization**

X-ray diffraction study of zinc oxide nanoparticles synthesised with *Trianthema portulacastrum* leaf extract exhibited unique peaks at  $2\theta$  values of  $31.72^\circ$ ,  $34.37^\circ$  and  $36.21^\circ$ , correlating with the (100), (002), and (101) crystallographic planes. The peaks are indicative of the hexagonal wurtzite structure of ZnO, as validated by JCPDS<sup>28</sup> card no. 36-1451. The predominance of the (101) peak indicates a favoured growth orientation along this plane, signifying anisotropic crystal formation. This growth behaviour frequently results in the creation of rod-like or hexagonal prism-shaped nanoparticles<sup>29</sup>. The lack of extraneous impurity peaks in the XRD pattern (Fig. 7) validates the high purity and crystallinity of the synthesised ZnO nanoparticles.

**Antimicrobial assay**

The zinc oxide nanoparticles synthesised with *Trianthema portulacastrum* (*Sharunai*) leaf extract exhibited diverse antibacterial efficacy against various microbes owing to their distinctive physicochemical characteristics. Nanoparticles effectively hinder microbial growth by generating reactive oxygen species (ROS), which induce oxidative stress that

damages bacterial cell membranes, proteins, and DNA, ultimately leading to cell death. The discrepancies in inhibitory zones relative to gentamicin are probably attributable to variations in the susceptibility of bacteria to ZnO-NPs. The greater inhibition noted against *Mycobacterium tuberculosis* (25 mm/mL) in comparison to gentamicin (22 mm/mL) indicates that ZnO-NPs efficiently target its cell wall structure. The diminished inhibition of *Candida albicans* (16 mm/mL) and *Fusarium* (18 mm/mL) in comparison to gentamicin suggests a comparatively reduced antifungal efficacy, potentially attributable to the thick fungal cell wall serving as a barrier (Fig. 8, 9). The differences in activity between *Gram-positive* (*Pneumococci*) and *Gram-negative* (*Escherichia coli*) bacteria show how cell wall composition affects susceptibility. The phytochemicals obtained from the *Sharunai* leaf extract may augment the antibacterial activity of ZnO-NPs, resulting in a synergistic effect. This highlights the capability of plant-mediated ZnO nanoparticles as environmentally acceptable and efficient antibacterial agents.

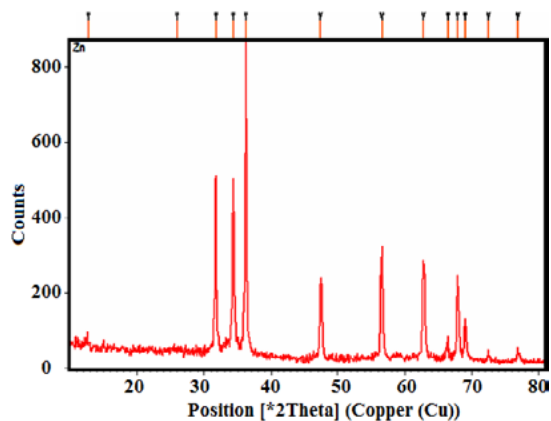


**Fig. 8. Comparative Analysis of Inhibition Zone**

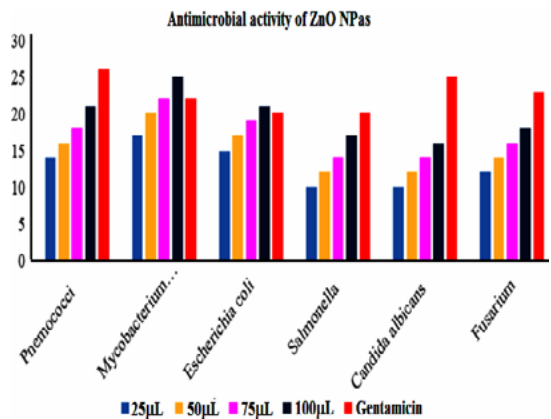
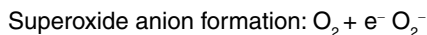


**Fig. 7. XRD studies for Zinc nanoparticles**

**Mechanism**

**Reactive Oxygen Species (ROS) generation:**

ROS such superoxide anions ( $O_2^-$ ), hydrogen peroxide ( $H_2O_2$ ), and hydroxyl radicals ( $\bullet OH$ ) are produced by ZnO-NPs, contributing to their antibacterial capabilities. ROS damage microbial cell components, killing them. The Fig. 9 illustrates the same.



**Release of Zinc Ions ( $Zn^{2+}$ )**

ZnO-NPs can release  $Zn^{2+}$  ions in aqueous environments. These ions can interact with microbial enzymes and proteins, disrupting essential metabolic pathways and further inhibiting microbial growth.

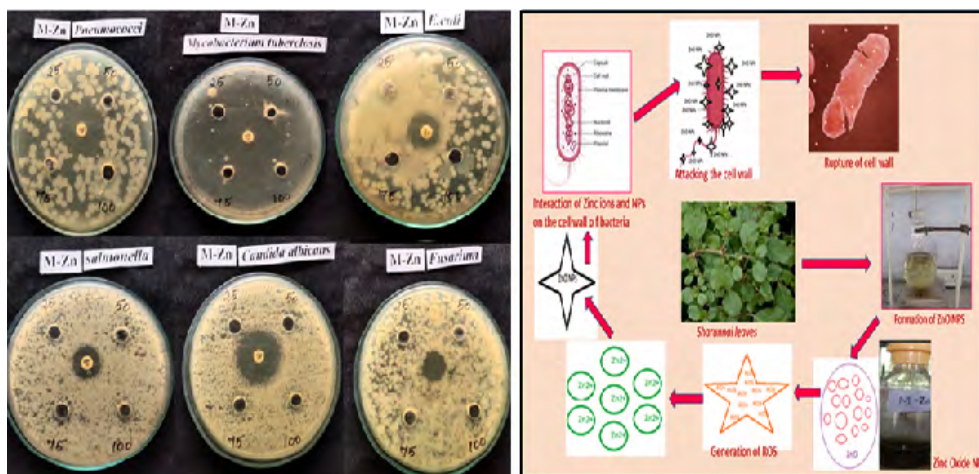
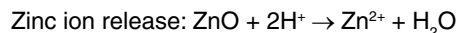


**Fig. 9. Antibacterial activity of the ZnO at different concentration and mechanism of Tp-ZnO NPS**

**CONCLUSION**

The effective green synthesis of ZnO nanoparticles utilising *Trianthema portulacastrum* extract illustrates a viable, non-toxic, and scalable alternative to traditional nanoparticle fabrication methods. This method utilises the plant's own phytochemicals-flavonoids, phenolics, and alkaloids-as bioreductants and stabilisers, resulting in the creation of precisely defined nanostructures with elevated purity and bioactivity. Comprehensive spectroscopic and morphological evaluations confirmed the structural integrity, functionalisation, and homogeneity of the nanoparticles. The biosynthesised ZnO nanoparticles exhibited significant antibacterial efficacy, especially against Gram-positive bacteria and *Mycobacterium tuberculosis*, underscoring their medicinal potential. The plant-based synthesis process guarantees minimal environmental impact and financial efficiency,

rendering it appropriate for large-scale production. This research advances the subject of green nanotechnology and establishes a scientific basis for the application of ethnomedicinal plants in sophisticated biomedical uses, including tailored antimicrobial delivery systems, wound healing, and biocompatible nanocomposites.

**ACKNOWLEDGMENT**

I thank the Management and the students for their support.

**Conflict of interests**

The authors declare that there is no conflict of interest.

**Author contributions**

All the authors contributed significantly to this manuscript, participated in reviewing/editing and approved the final draft for publication.

**REFERENCES**

1. Yadav, A.; Kumar, H.; Kumar, P.; Rani, G.; Maken, S., *J. Mol. Struct.*, **2025**, *1325*, 141017. <https://doi.org/10.1016/j.molstruc.2024.141017>

2. Li, K.; Ren, Y.; Lin, D.; Tong, M.; Yang, B.; Xiao, F.; Hou, Y.; Lu, Y.; He., *J. Inorg. Chem. Commun.*, **2025**, *151*, 114577. <https://doi.org/10.1016/j.inoche.2025.114577>
3. Ilavenil, K. K.; Senthilkumar, V.; Kasthuri, A., *Discov. Catal.*, **2025**, *2*, 3. <https://doi.org/10.1007/s44344-025-00007-6>
4. Mahmoud, A. E. D.; Stolle, A.; Stelter, M., *ACS Sustainable Chem. Eng.*, **2018**, *6*, 25. <https://doi.org/10.1021/acssuschemeng.8b00147>
5. Ashwin, B. M.; Yardily, A., & Dennison, M. S., *Discover Applied Sciences.*, **2025**, *7*(3), 177. <https://doi.org/10.1007/s42452-025-06563-8>
6. Mellinas, C.; Jiménez, A.; Garrigós, M. C., *Molecules.*, **2019**, *24*, 4048. <https://doi.org/10.3390/molecules24224048>
7. Naiel, B., Fawzy, M., Halmy, M. W. A., & Mahmoud, A. E. D. *Scientific Reports.*, **2022**, *12*(1), 20370. <https://doi.org/10.1038/s41598-022-24805-2>
8. Aldeen, T. S.; Mohamed, H. E. A.; Maaza, M., *J. Phys. Chem. Solids.*, **2022**, *160*, 110313. <https://doi.org/10.1016/j.jpcs.2021.110313>
9. Mahmoud, A. E. D.; El-Maghrabi, N.; Hosny, M., & Fawzy, M., *Environ. Sci. Pollut. Res.*, **2022**, *29*(59), 89772–89787. <https://doi.org/10.1007/s11356-022-21871-x>
10. Golzarnezhad, F.; Allahdou, M.; Mehravaran, L., & Naderi, S., *Discover Applied Sciences.*, **2025**, *7*(3), 196. <https://doi.org/10.1007/s42452-025-06623-z>
11. Chabattula, S. C.; Gupta, P. K.; Tripathi, S. K.; Gahtori, R.; Padhi, P.; Mahapatra, S.; Biswal, B. K., *Mater. Today Chem.*, **2021**, *22*, 100618. <https://doi.org/10.1016/j.mtchem.2021.100618>
12. Rauf, M. A.; Oves, M.; Rehman, F. U.; Khan, A. R.; Husain, N., *Biomed. Pharmacother.*, **2019**, *116*, 108983. <https://doi.org/10.1016/j.biopha.2019.108983>
13. Agarwal, H.; Menon, S.; Shanmugam, V. K., *Surf. Interfaces.*, **2020**, *19*, 100521. <https://doi.org/10.1016/j.surfin.2020.100521>
14. Ganesan, L.; Arumugam, M.; Maluventhen, V., *Biomed. Mater. Devices.*, **2025**. <https://doi.org/10.1007/s44174-025-00346-w>
15. Xia, Y.; Yang, P.; Sun, Y.; Wu, Y.; Mayers, B.; Gates, B.; Yin, Y.; Kim, F.; Yan, H., *Adv. Mater.*, **2003**, *15*, 353–389. <https://doi.org/10.1002/adma.200390087>
16. Lahoti, R.; Carroll, D., *Next Res.*, **2025**, *1*, 100164. <https://doi.org/10.1016/j.nexres.2025.100164>
17. Babayevska, N.; Przysiecka, Ł.; Iatsunskyi, I.; Nowaczyk, G.; Jarek, M.; Janiszewska, E., & Jurga, S., *Sci. Rep.*, **2022**, *12*(1), 8148. <https://doi.org/10.1038/s41598-022-12134-3>
18. Gaddeyya, G.; Kumar, R. P. K., *J. Crop Weed.*, **2015**, *11*, 47–54.
19. Falade, T.; Ishola, I. O.; Akinleye, M. O.; Oladimeji-Salami, J. A.; Adeyemi, O. O., *J. Ethnopharmacol.*, **2019**, *238*, 111831. <https://doi.org/10.1016/j.jep.2019.111831>
20. Poddar, S.; Ghosh, P.; Sarkar, T.; Sarkar, A.; Choudhury, S.; Chatterjee, S., *J. Pharm. Sci. Res.*, **2020**, *12*(7), 899–903.
21. Ghosh, P.; Chatterjee, S.; Das, P.; Banerjee, A.; Karmakar, S.; Mahapatra, S., *Int. J. Pharm. Sci. Res.*, **2019**, *10*(4), 1605–1612. [https://doi.org/10.13040/IJPSR.0975-8232.10\(4\).1605-12](https://doi.org/10.13040/IJPSR.0975-8232.10(4).1605-12)
22. Yamaki, J.; NagulapalliVenkata, K. C.; Mandal, A.; Bhattacharyya, P.; Bishayee, A., *J. Integr. Med.*, **2016**, *14*(2), 84–99. [https://doi.org/10.1016/S2095-4964\(16\)60247-9](https://doi.org/10.1016/S2095-4964(16)60247-9)
23. Jaiswal, V.; Lee, H.-J. *Plants.*, **2025**, *14*(3), 349. <https://doi.org/10.3390/plants14030349>
24. Chowdhury, V.; Shristy, N. T.; Rahman, M. H.; Chowdhury, T. A. Dhaka Univ. *J. Pharm. Sci.*, **2022**, *21*(1), 33–43. <https://doi.org/10.3329/dujps.v21i1.60394>
25. Laasya, T. P. S.; Thapliyal, S.; Goel, K. K.; Kumar, B.; Poduri, R.; Joshi, G., *Sep. Sci. Plus.*, **2024**, *7*(2), 2300140. <https://doi.org/10.1002/sscp.202300140>
26. Okolo, S. C.; Habila, J. D.; Hamisu, I. *Niger. J. Chem. Res.*, **2024**, *29*(2), 115–121. <https://doi.org/10.4314/njcr.v29i2.4>
27. Saputra, I. S.; Nurfani, E.; Fahmi, A. G.; Saputro, A. H.; Apriandanu, D. O. B.; Annas, D.; Yulizar, Y., *Vacuum.*, **2024**, *227*, 113434. <https://doi.org/10.1016/j.vacuum.2024.113434>
28. Arefi, M. R.; Rezaei-Zarchi, S. R., *Int. J. Mol. Sci.*, **2012**, *13*(4), 4340–4350. <https://doi.org/10.3390/ijms13044340>
29. Cao, D.; Gong, S.; Shu, X., *Nanoscale Res. Lett.*, **2019**, *14*, 210. <https://doi.org/10.1186/s11671-019-3038-3>